Journal of Molecular Modeling (2019) 25:142
https://doi.org/10.1007/s00894-019-4026-3

ORIGINAL PAPER

Adsorption behavior of mercuric oxide clusters on activated carbon and the effect of SO_2 on this adsorption: a theoretical investigation

Zhengyang Gao[1] · Xiaoshuo Liu[1] · Ang Li[1] · Chuanzhi Ma[1] · Xiang Li[1] · Xunlei Ding[2] · Weijie Yang[1]

Received: 15 January 2019 / Accepted: 4 April 2019

Abstract

The release of mercury (Hg) species from coal-fired power plants has attracted increasing concern, and the development of an efficient and economical method to control Hg species emission from such plants is urgently required. Activated carbon is a compelling sorbent for the elimination of mercury species from flue gas, but the adsorption mechanism of mercuric oxide clusters on carbonaceous materials is still unclear. Therefore, the adsorption characteristics of mercuric oxide clusters on activated carbon were investigated systematically utilizing density functional theory in this work. It was found that mercuric oxide clusters are chemically adsorbed on activated carbon, and that the pre-adsorption of SO_2 on the activated carbon leads to complicated mercuric oxide cluster adsorption behavior due to an irregular distribution of the electrostatic potential on the surface of the carbonaceous material. Thermodynamic analysis indicated that the adsorption energy of SO_2 on activated carbon is lower than that of mercuric oxide clusters in the temperature range 298.15–1000 K. Competitive adsorption analysis suggested that mercuric oxide clusters are at least $10^{8.11}$ times more likely than SO_2 to be adsorbed on activated carbon.

Keywords Activated carbon · Mercuric oxide clusters · SO_2 · Electrostatic potential · Competitive adsorption

Introduction

Mercury pollution is regarded as particularly dangerous due to its high toxicity, the ease with which it becomes concentrated in organisms, and the difficulties involved in removing this pollution [1, 2]. The main anthropogenic source of mercury pollution is currently coal-fired power plants [3], causing global concern over the release of mercury from stationary combustion sources. Therefore, it is important to eliminate mercury pollution from power stations as urgently as possible.

✉ Zhengyang Gao
gaozhyan@163.com

✉ Xiaoshuo Liu
liuxiaoshuo@ncepu.edu.cn

✉ Xunlei Ding
dingxl@ncepu.edu.cn

[1] School of Energy and Power Engineering, North China Electric Power University, Baoding 071003, China

[2] School of Mathematics and Physics, North China Electric Power University, Beijing 102206, China

There are three types of mercury in flue gas: elemental mercury (Hg^0), oxidized mercury (Hg^{2+}), and particulate-bound mercury (Hg^p) [4]. While there has been a great deal of research into Hg^0 removal [5–10], the elimination of Hg^{2+} has barely been studied. However, it is very important to remove Hg^{2+} from flue gas because when the gas passes through the selective catalytic reduction (SCR) system, some of the Hg^0 present is oxidized to Hg^{2+} by catalysts [11]; indeed, for coal-fired power plants that burn bituminous coal, as much as 98% of the Hg^0 is oxidized [12]. Moreover, the catalytic oxidation of Hg^0 by oxygen has been viewed as a promising method of controlling mercury pollution [11, 13–17], but this process converts most of the Hg^0 in flue gas to Hg^{2+}, making it even more important to develop techniques for eliminating Hg^{2+}.

There is no specialized method for removing Hg^{2+} in coal-fired power plants, but it can be removed together with other toxic chemicals. Some of the Hg^{2+} can be adsorbed on carbonaceous materials such as activated carbon to form Hg^p during the Hg^0 removal process; the Hg^p can then be removed by an electrostatic precipitator system (ESPS) or fabric filters (FF). Hg^{2+} vapor can also be removed from the desulfurization slurry using a wet flue gas desulfurization (WFGD) system, which makes use of its high solubility in water [7]. Although some research into the adsorption of Hg^{2+} by a WFGD system was recently

Published online: 01 May 2019

published [18], a corresponding investigation of the mechanism for the removal of Hg^{2+} on activated carbon is still awaited.

Activated carbon is considered a perfect sorbent for flue gas due to its low cost and excellent gas adsorption properties, and it has been widely used to remove H_2S [19, 20], arsenic species [21], Hg^0 [22–24], and NO_x [25] in real-world applications. Moreover, quantum chemistry supplies wonderful methods that can demonstrate the excellent adsorption characteristics of activated carbon at the molecular level. Shen et al. [26] carried out theoretical calculations of the adsorption of H_2S on a carbonaceous surface, and they found that the adsorption energy of H_2S on the sorbent could reach −664.9 kJ/mol. Gao et al. [27] investigated the adsorption of As_2O_3 on carbonaceous chars, and they observed that a zigzag char possessed an outstanding adsorption capacity for As_2O_3, with a high adsorption energy of −480.20 kJ/mol. Zhang et al. [28] found, using a quantum chemistry method, that the adsorption energy of NO on activated carbon reached −178.5 kJ/mol. These results suggest that activated carbon could also have a high capacity to adsorb mercuric oxide clusters.

In order to gain a comprehensive understanding of the mechanism for the adsorption of mercuric oxide clusters on different activated carbons, and to facilitate the development of guidelines for the elimination of mercuric oxide, we performed quantum chemistry calculations of the adsorption of mercuric oxide clusters on activated carbon. First, the adsorption energies of various mercuric oxide clusters on different activated carbons were obtained. Second, coals with high mercury contents tend to be high-sulfur coals [29], so the influence of the pre-adsorption of SO_2 on the adsorption of mercuric oxide clusters on activated carbon was researched for various stable configurations of SO_2-adsorbed activated carbon. The electrostatic potential (ESP) distribution was calculated to characterize the activity of the carbonaceous surface after it had been modified by the adsorption of SO_2. Third, thermodynamic analysis was performed across a wide temperature range (between 298.15 K and 1000 K) with the intention of investigating how the adsorption energy varies with the temperature. Lastly, based on this thermodynamic analysis, a detailed analysis of the competitive adsorption of SO_2 and mercuric oxide clusters as a function of temperature was conducted using the Boltzmann distribution function (B_{df}) in order to gain a deeper understanding of the adsorption of mercuric oxide clusters on activated carbon. The results of this work not only reveal the mechanism for the removal of mercuric oxide clusters by activated carbon, but they also lay the foundations for the further study of mercury elimination using Hg^0 catalytic oxidation technology in coal-fired power plants that burn high-sulfur coal.

Computational details

Density functional theory (DFT) has been shown to be a favorable choice for calculating structural properties as it provides a good balance between computational efficiency and accuracy [6]. In this work, the structural optimizations and frequency calculations for all molecules were performed at the B3LYP/6-31G(d) level (except for Hg, for which the SDD basis set was used) and implemented using the Gaussian09 software package [30], and related single-point energy calculations were carried out at the PWPB95-D3(BJ) [31] (double hybrid density functional)/def2-TZVP (all-electron basis sets for elements in the first four rows) level utilizing the ORCA 3.0.1 software package [32] to obtain accurate electronic energy information. The B3LYP/6-31G(d) level was selected as it has been widely applied in studies of the adsorption of small gas molecules on carbonaceous materials [28, 33, 34], and the Stuttgart group basis set (SDD) was utilized for Hg atoms in order to account for relativistic effects [35]. The PWPB95-D3 (BJ)/def2-TZVP level was employed to derive the single-point energy because of its high accuracy when examining carbonaceous materials [27, 36, 37]. Frequency analysis was performed to check for imaginary frequencies and obtain the zero point energy (ZPE) and corresponding thermodynamic quantities [38].

The ground state of each structure was determined via single-point energy calculations for several spin multiplicities. The structure with the lowest Gibbs free energy was considered the ground state (i.e., the most thermodynamically stable configuration of the molecular system of interest [35]). The Gibbs free energy can be obtained by adding the thermal free energy obtained at the B3LYP/6-31G(d) level to the electronic energy obtained at the PWPB95-D3(BJ)/def2-TZVP level, and it is worth mentioning that the temperature was always maintained at 298.15 K in our calculations, except in some thermodynamic calculations.

When a gas molecule is adsorbed on the surface of activated carbon, the overall process tends to be exothermic, and the heat released is defined as the adsorption energy, which can be calculated as follows [39]:

$$\Delta G_{\text{ads}} = G_{AB} - G_A - G_B.$$

Here, G_{AB} represents the Gibbs free energy of the whole system AB, and G_A and G_B are the Gibbs free energies of the adsorbate and the activated carbon, respectively. There are two types of adsorption. If the value of ΔG_{ads} is in the range from −0.3 to −0.1 eV, the absorption can be classified as physical absorption. If its value is more negative than −0.5 eV, it is considered to be chemical adsorption [40]. Basically, a more negative value of ΔG_{ads} corresponds to a stronger adsorption energy.

Thermodynamic analysis was carried out from 298.15 K to 1000 K, reflecting the variation in the temperature of the flue gas from boiler outlet to chimney [41]. The Boltzmann distribution function was used to probe the competitive adsorption of mercuric oxide clusters and SO_2 quantitatively across the temperature range of interest. The Boltzmann distribution

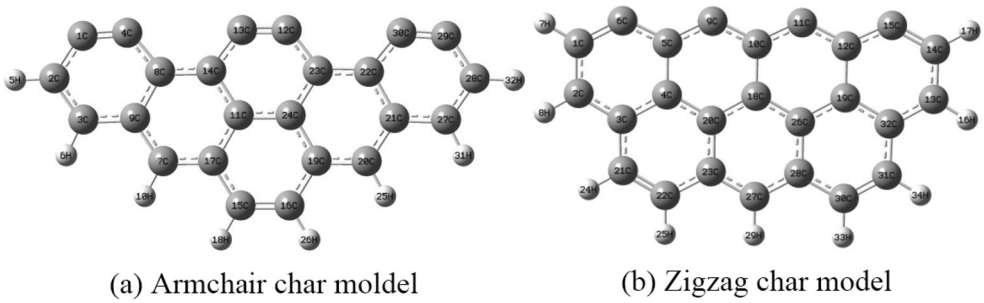

(a) Armchair char moldel (b) Zigzag char model

Fig. 1 Optimized models of the activated carbon surface employed in the present work

function represents the adsorption probability ratio for two molecules (A and B) competing for the same active site, which can be determined by the following equation [42, 43]:

$$B_{\mathrm{df}} = \frac{N_{\mathrm{A}}}{N_{\mathrm{B}}} = \exp\left(-\frac{G(\mathrm{A}) - G(\mathrm{B})}{kT}\right).$$

Here, G(A) and G(B) are the ground-state Gibbs free energies (in eV) of molecules A and B, respectively; k is the Boltzmann constant (8.62×10^{-5} eV K^{-1}); and T is the temperature of the molecular system (in K). Obviously, the greater the value of B_{df}, the higher the probability that molecule A is adsorbed on the sorbent instead of molecule B. Analyzing B_{df} allows us to quantitatively explore, at a molecular level, the competition between the mercuric oxide clusters and SO_2 to bind to the carbon.

Results and discussion

Modeling the surface of activated carbon

In this work, a model consisting of finite benzene clusters in a monolayered graphitic structure (a common simplified model of activated carbon) was adopted to describe the surface of the carbonaceous material. Models similar to this one have been successfully utilized in many investigations [26, 28, 33, 34, 39, 44, 45], and have yielded accurate results in studies of Hg species [3, 7, 26, 45, 46]. It has also been shown by solid-state ^{13}C NMR that activated carbon consists of clusters of 3–7 benzene rings [26, 47], and plenty of investigations have indicated that the size of the benzene clusters in the activated carbon has little effect on its capacity to adsorb other molecules, although the edge shape of the activated carbon is known to play an important role in gas adsorption [26, 27, 48]. Furthermore, Montoya et al. [49] argued that the reactivity of a carbonaceous surface depends mainly on the local structure around the active sites; for instance, whether an armchair or a zigzag structure is present. Hence, in order to provide enough adsorption sites and ensure that our results are comprehensive, we examined two models: one with six benzene rings in an armchair structure, and the other with seven benzene rings in a zigzag structure. Unsaturated carbon atoms in the models acted as the active sites, and other carbon atoms at the edges of the models were saturated completely with hydrogen atoms to avoid boundary effects [50]. Figure 1 shows the two models of activated carbon, namely the armchair and zigzag models, after geometry optimization.

Moreover, the average C–C bond lengths and C–C–C bond angles were counted after geometry optimization. For the armchair model, bond lengths were 1.40 Å on average and the mean C–C–C bond angle was 120.1°. The average C–C bond length was 1.41 Å and the mean C–C–C bond angle was 120.0° for the zigzag model. These values are very close to the corresponding experimental data [51], indicating that our models are reasonable.

Adsorption of mercuric oxide clusters on activated carbon

Mercuric oxide clusters tend to consist of 1–4 HgO molecules [52], and considering the complicated chemical nature of flue gas

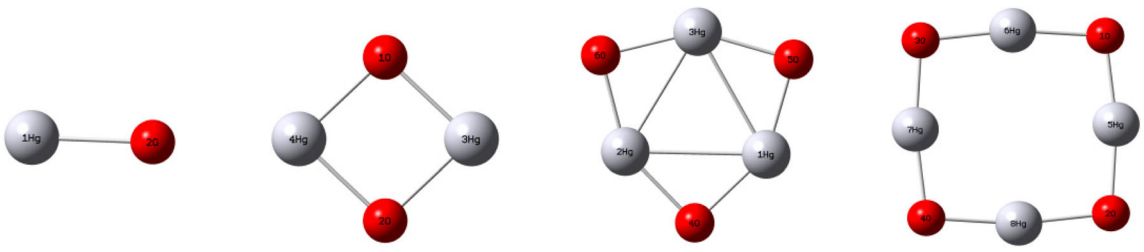

(a) HgO (b) Hg_2O_2 (c) Hg_3O_3 (d) Hg_4O_4

Fig. 2 Models of the mercuric oxide clusters Hg_xO_x (x = 1–4)

Table 1 Comparison of the average Hg–O bond length for each mercuric oxide cluster calculated in our work with the corresponding average bond length obtained in a previous study

Cluster	Mean Hg–O bond length (Å)
HgO	2.26 (2.04 [52])
Hg_2O_2	2.21 (2.24 [52])
Hg_3O_3	2.09 (2.17 [52])
Hg_4O_4	2.03 (2.34/2.19 [52])

and the wide range of temperatures that occur in boilers, it is necessary to take each mercuric oxide cluster size into consideration. Various configurations of mercuric oxide clusters were considered, and the stablest—i.e., those with the lowest ground-state energies—were selected for this investigation, as

Table 2 Adsorption energies of Hg_nO_n clusters on activated carbon structures

Configuration	E_{ads} (eV)	Configuration	E_{ads} (eV)
Armchair-HgO-1	−1.47	Zigzag-HgO-1	−1.67
Armchair-HgO-2	−3.21	Zigzag-HgO-2	−5.40
Armchair-$(HgO)_2$–1	−6.02	Zigzag-$(HgO)_2$–1	−6.50
Armchair-$(HgO)_2$–2	−1.03	Zigzag-$(HgO)_2$–2	−3.18
Armchair-$(HgO)_3$–1	−5.58	Zigzag-$(HgO)_3$–1	−9.49
Armchair-$(HgO)_3$–2	−6.75	Zigzag-$(HgO)_3$–2	−5.57
Armchair-$(HgO)_4$–1	−2.97	Zigzag-$(HgO)_4$–1	−7.75
Armchair-$(HgO)_4$–2	−3.37	Zigzag-$(HgO)_4$–2	−4.93

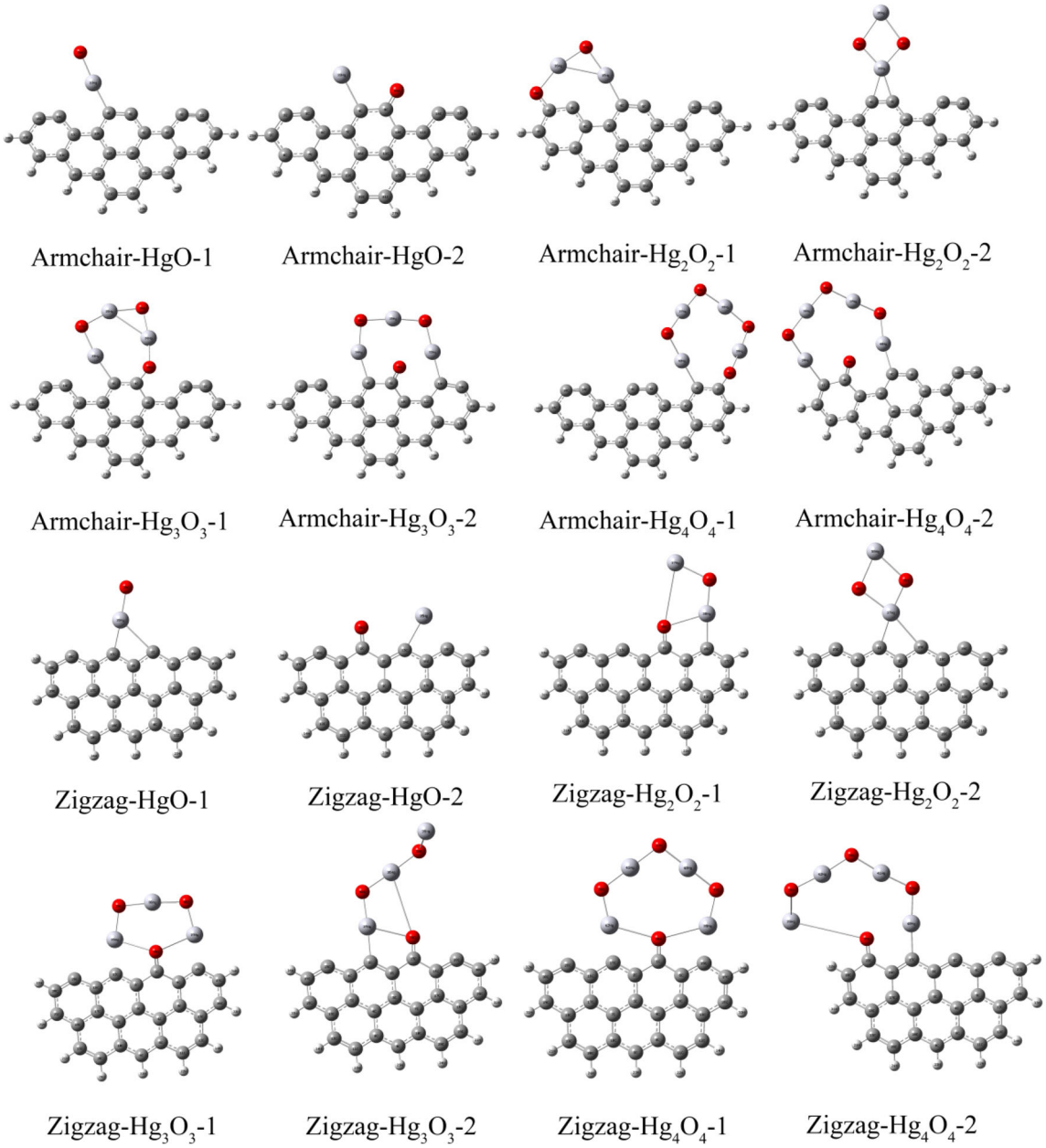

Fig. 3 Configurations of Hg_nO_n (n = 1–4) clusters adsorbed on activated carbon

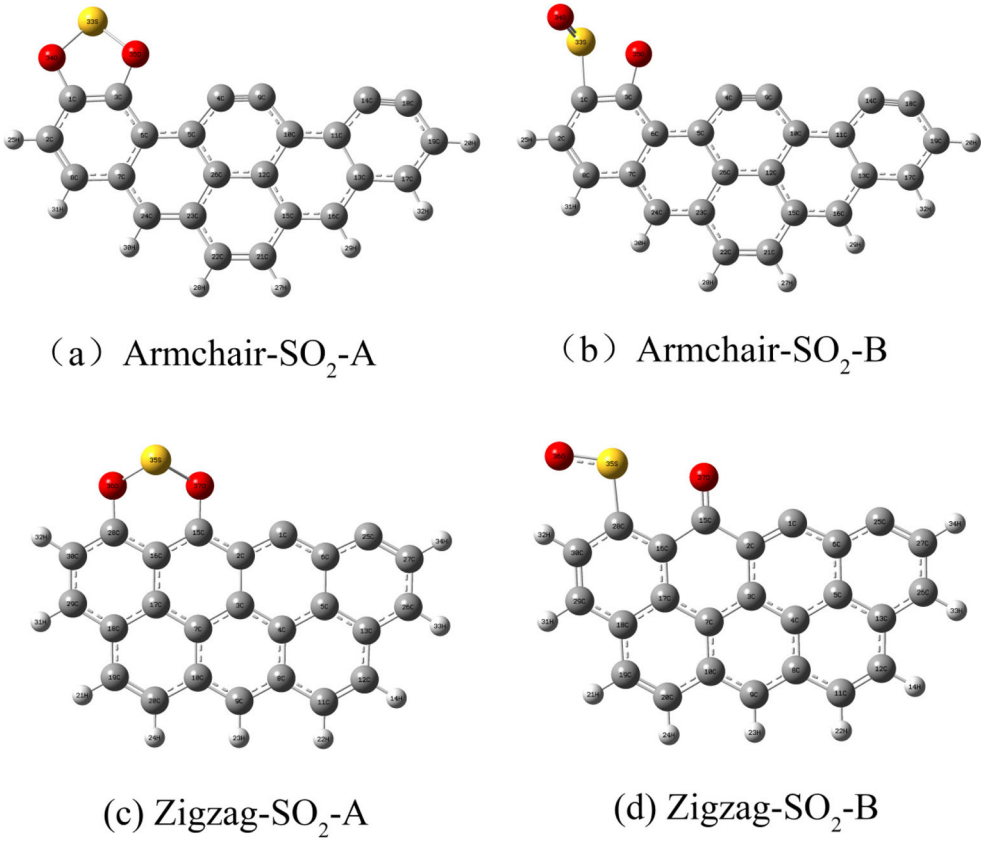

Fig. 4 Four configurations for the adsorption of SO_2 on activated carbon

shown in Fig. 2. The structures we obtained were found to be highly consistent with previously reported data on these clusters, as shown in Table 1.

To gain useful insight into the adsorption of mercuric oxide clusters on activated carbon, we considered various adsorption sites and all possible adsorption orientations of the mercuric oxide clusters on the carbonaceous surface. Sixteen stable adsorption configurations were explored for the armchair and zigzag activated carbon models, as shown in Fig. 3; detailed parameters are listed in Table 2. It is clear from this table that all possible adsorption configurations of mercuric oxide clusters on armchair activated carbon can be categorized as chemical adsorption due to the considerable adsorption energies involved (exceeding −1.03 eV). For the eight adsorption configurations on zigzag activated carbon, the adsorption energies were generally even larger than those associated with armchair activated carbon, indicating that the zigzag activated carbon is more active than the armchair activated carbon. This conclusion was also drawn in previous studies [53, 54], and can be explained by theoretical calculations indicating that the zigzag carbon has sextet spin in the ground state whereas the armchair carbon has singlet spin in the ground state, pointing to a closed-shell system in the ground-state armchair structure and an open-shell system in the ground state of the zigzag structure. The existence of unpaired electrons in the open-shell system leads to enhanced surface activity.

Compared to the adsorption of Hg^0 on a carbonaceous surface, the interactions between the activated carbon structures and the mercuric oxide clusters were found to be pretty strong, which can be attributed to the charge on the Hg atoms in the mercuric oxide clusters. The strong adsorption of mercuric oxide clusters by activated carbon suggests that activated carbon could be a great candidate for use as a sorbent for mercuric oxide clusters, and it supports the argument that the mercuric oxide clusters generated by SCR catalysts could be adsorbed on activated carbon and then removed via ESP/FF, rather than retaining the Hg^{2+} in a vapor state so that it can be removed using a WFGD system.

Effect of the pre-adsorption of SO_2 on the adsorption of mercuric oxide clusters by activated carbon

The pre-adsorption of a small amount of SO_2 is actually beneficial to the adsorption of Hg^0 [55], so we wanted to investigate how the pre-adsorption of SO_2 would affect the adsorption of mercuric oxide clusters by activated carbon. In this research, a study of the pre-adsorption of SO_2 was first carried out, and SO_2 molecules were then adsorbed in four configurations denoted Armchair-SO_2-A, Armchair-SO_2-B, Zigzag-SO_2-A, and Zigzag-SO_2-B, respectively (see Fig. 4), with adsorption energies of −1.80, −1.60, −2.89, and − 3.48 eV, respectively. Based on these four poses of SO_2 on activated

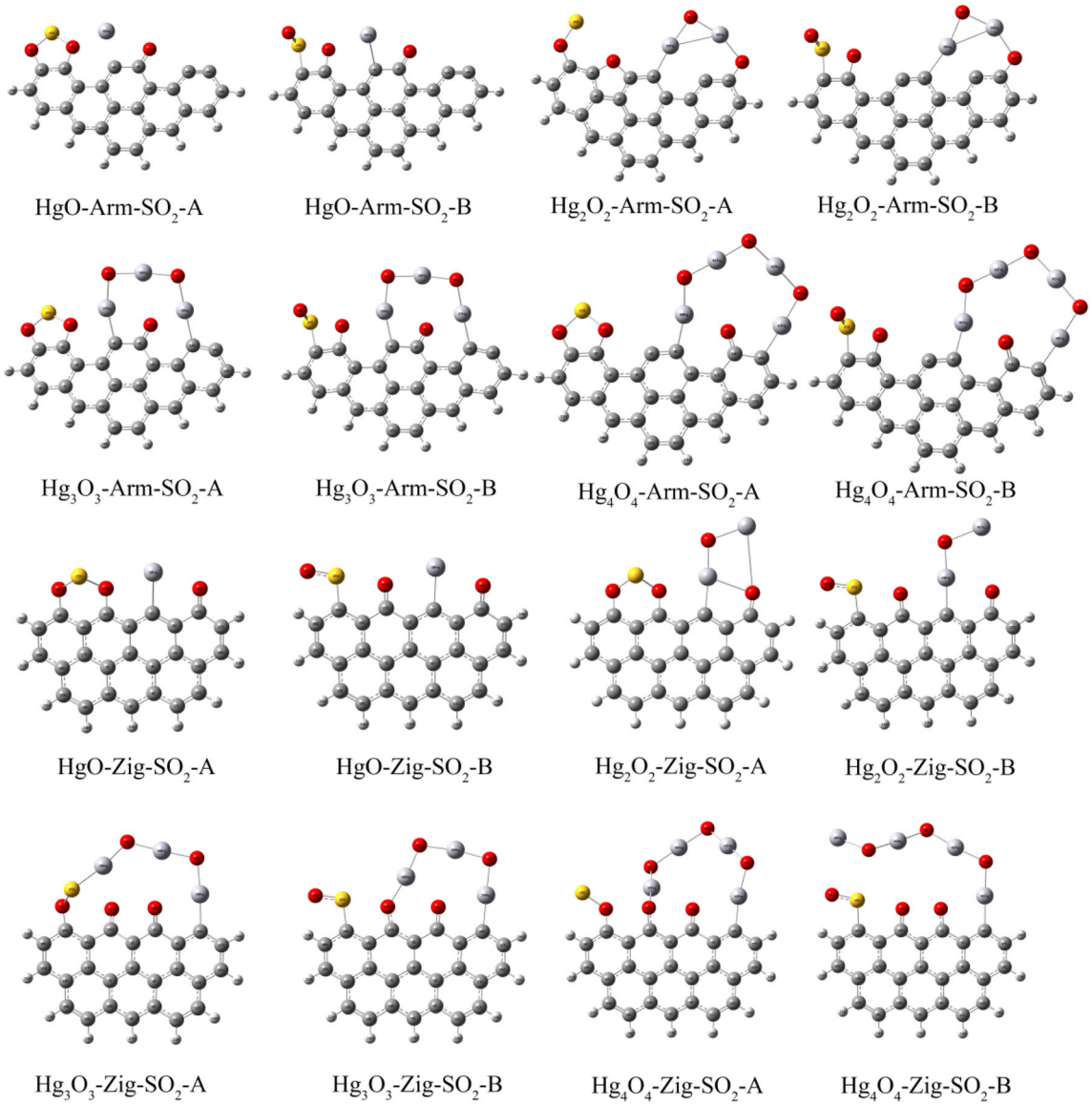

Fig. 5 Scenarios for the adsorption of mercuric oxide clusters on SO_2-modified activated carbon

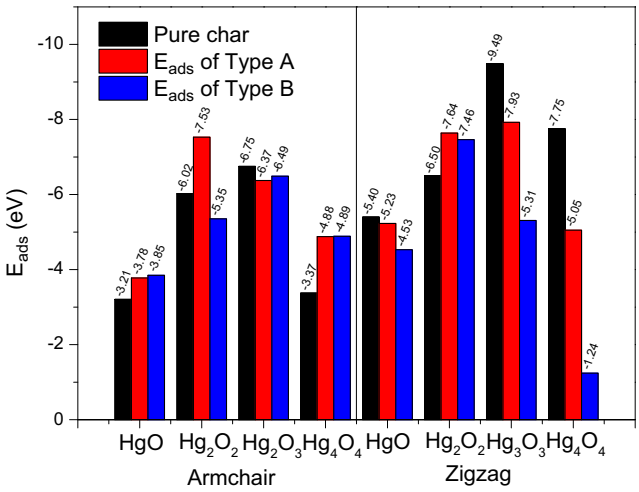

Fig. 6 Adsorption energies of the Hg_nO_n clusters on activated carbon and SO_2-modified activated carbon

carbon, 16 scenarios for the adsorption of mercuric oxide clusters on SO_2-modified activated carbon were examined (see Fig. 5), focusing on adsorption energies as well as electrostatic potentials.

As shown in Fig. 6, the adsorption energies of the mercuric oxide clusters on the pure armchair/zigzag activated carbon and the SO_2-modified armchair/zigzag activated carbon were obtained for the most stable configurations. The results indicated that the pre-adsorption of SO_2 had a complicated effect on the adsorption of the mercuric oxide clusters. The adsorption of the clusters can be enhanced or suppressed depending on the configuration for the adsorption of the SO_2 on activated carbon, the edge structure of the activated carbon model, and the particular mercuric oxide cluster considered. This result is quite different from the adsorption behavior of Hg^0 on SO_2-modified activated carbon. It was also noted that the

adsorption energies of mercuric oxide clusters on the Armchair-SO_2-A and Zigzag-SO_2-A structures are similar to or even far greater than those for the clusters on the Armchair-SO_2-B and Zigzag-SO_2-B structures, indicating that the configurations involving direct O–O bonding to the activated carbon (type A) are more active than those involving O–S bonding or the binding of O to the carbonaceous surface (type B).

In order to further explain how the pre-adsorption of SO_2 affects the adsorption capacity of the activated carbon surface, we examined the electrostatic potential (ESP) distribution. ESP analysis of molecular surfaces is useful because it allows the interactions between molecules to be predicted and described [37, 56]. It has therefore been applied to characterize the activities of carbonaceous systems [57]. Furthermore, ESP analysis can be employed to conveniently explore such systems qualitatively when used in conjunction with the wavefunction analysis software Multiwfn [58]. Therefore, an investigation of ESP at the activated carbon surface was conducted to gain a deeper understanding on the activities of the various activated carbon surfaces as well as the relationship between the ESP distribution and the adsorption energy.

The surface area ratios for various ESP values on each activated carbon surface and each SO_2-modified activated carbon surface are presented in Fig. 7a. The absolute values of ESP shown in this plot correlate directly with the adsorption ability of the sorbent. A plot of the cumulative sum of the surface area ratios (as shown in Fig. 7a) with increasing ESP for each activated carbon system is provided in Fig. 7b. The shallower the curve representing the cumulative sum of the surface area ratios, the greater the fraction of the activated carbon surface that exhibits high ESP. In Fig. 7b, the curves for zigzag activated carbon are always below the corresponding curves for armchair activated carbon, implying that the zigzag carbon is always more active than the armchair carbon, in good agreement with the conclusion we drew based upon the adsorption energies, thus indicating that the ESP distribution could be a useful descriptor of activated carbon activity. Moreover, we observed that more than 60% of the surface of each activated carbon structure presented ESP values ranging from −0.3 to 0.3 eV. Considering the fact that we sealed the active sites on three sides of the activated carbon model, allowing active sites to occur on only one side of the model, it is reasonable to speculate that the areas with absolute ESP values above 0.3 eV should belong to the regions with accessible active sites on the edge of the model. Besides, it is clear that in the surface regions with absolute ESP values between 0.3 eV and 1.5 eV, the area ratio sum curves cross over in some cases, indicating that one of the activated carbon structures changes from being less to being more surface active than another activated carbon structure. Therefore, none of these activated carbon models show unusually high or low adsorption ability across the whole surface area, although the adsorption capacity of edge sites differs significantly between activated carbon structures. The phenomenon of crossing area ratio sum curves for the activated carbon surfaces is likely to be one of the main reasons why the pre-adsorption of SO_2 did not always improve the adsorption capacities of the activated carbon structures for mercuric oxide clusters, in contrast to the adsorption of Hg^0. Of course, this may also be attributable to various other reasons, such as differences in adsorption sites and intermolecular binding, or huge distortions during the adsorption process.

Thermodynamic analysis

The variation in the adsorption energy of each mercuric oxide cluster on each activated carbon structure was then investigated to explore thermodynamic effects on this adsorption.

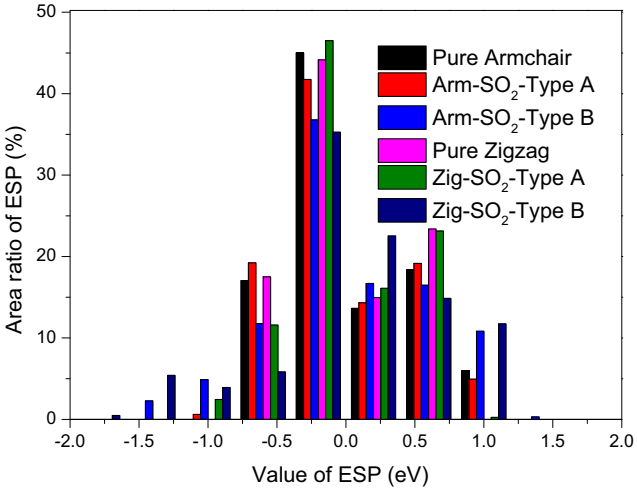

(a) The area ratio for the ESP value of activated carbon models

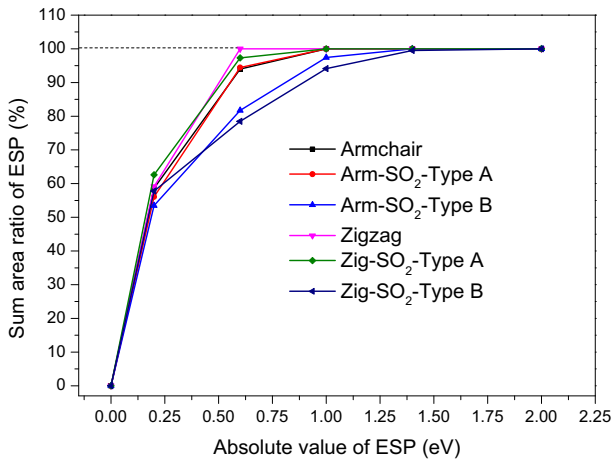

(b) Cumulative sum of ESP area ratios of activated carbon models

Fig. 7 ESP distributions for different activated carbon models. **a** Plot of the surface area ratios of various ESP values for the activated carbon models. **b** Plot showing curves representing the cumulative sum of the surface area ratios (as depicted in **a**) as a function of ESP value for each activated carbon model

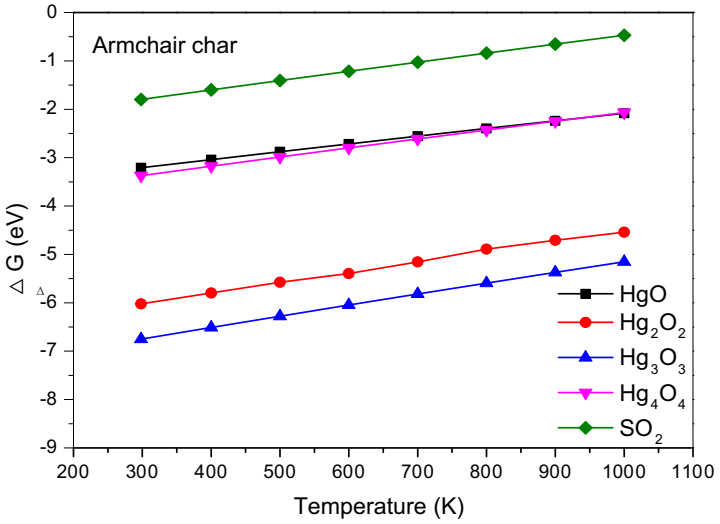

(a) The adsorption energies with different temperatures for Armchair activated carbon

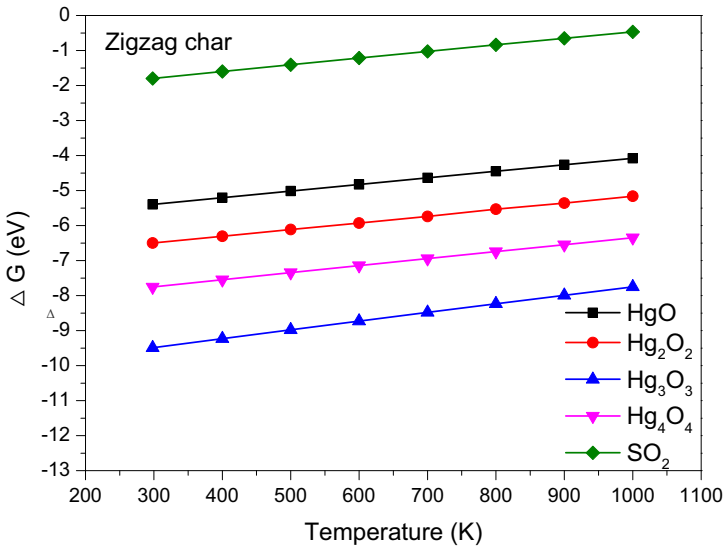

(b) The adsorption energies with different temperatures for Zigzag activated carbon

Fig. 8 Adsorption energy as a function of temperature. **a** Plot of adsorption energies of mercuric oxide clusters on armchair activated carbon structures versus temperature. **b** Plot of adsorption energies of mercuric oxide clusters on zigzag activated carbon structures versus temperature

Considering the range of temperatures experienced by flue gas from boiler outlet to chimney in coal-fired boilers, we selected a temperature range of 298.15–1000 K for our thermodynamic study. Based on the adsorption energy trends shown in Fig. 8, it is clear that the strength of the interactions between mercuric oxide clusters/SO_2 and the activated carbon structures is inversely proportional to the temperature. Recently, the development of SCR technology and the catalytic oxidation of nitrogen oxides and mercury at low temperatures (298.15–550 K) have become hot research topics in the fields of pollutant treatment and catalytic science, and the high adsorption capacity of activated carbon for mercuric oxide clusters at low temperatures make it a great candidate for use as a sorbent. Moreover, it was found that the adsorption strengths of the mercuric oxide clusters and SO_2 on the armchair activated carbon decrease in the order $(HgO)_3 > (HgO)_2 > (HgO)_4 > HgO > SO_2$; the corresponding order for adsorption on zigzag activated carbon is $(HgO)_3 > (HgO)_4 > (HgO)_2 > HgO_2 > SO_2$. Thus, the adsorption energy of SO_2 on the carbon is relatively weak, and any mercuric oxide cluster would win a competition with SO_2 to bind at an active site on activated carbon.

In previous literature, the existence of a large amount of SO_2 was reported to block Hg^0 removal [59]. The corresponding influence of competitive adsorption on the adsorption of mercuric oxide clusters is discussed in the next section.

Analysis of the competitive adsorption of mercuric oxide clusters and SO_2

Though the adsorption energies of mercuric oxide clusters on activated carbon are far greater than the adsorption energy of SO_2 on activated carbon, the very different volume fractions of mercury species (0.1 ppm [11]) and SO_2 (50 ppm to 17,190 ppm [60]) in flue gas could significantly alter the presumed order of adsorption (i.e., that mercury species are adsorbed before SO_2). In order to probe the mechanism for the adsorption of these species on activated carbon and to investigate the impact of the volume fractions of these species in flue gas on their competitive adsorption behavior, quantitative research into the adsorption probabilities of mercuric oxides by SO_2 was carried out utilizing B_{df}. Gao et al. [42] investigated the co-adsorption of NO and CO molecules on various graphenes (catalyzed by single iron atoms) using B_{df} and obtained favorable values for the adsorption probabilities of NO and CO on different sorbents, indicating that B_{df} could be a useful descriptor of competitive adsorption on carbonaceous materials. In flue gas, the amount of SO_2 is 500–171,900 ($10^{2.70}$–$10^{5.24}$) times greater than the amount of mercury species. We have plotted the relationship between the logarithm of B_{df} and the temperature in Fig. 9, and the results show that the logarithm of B_{df} always declines with increasing temperature for adsorption on armchair and zigzag activated carbon structures. This is consistent with the tendency for the adsorption energy to increase as the temperature drops. The lowest values for the logarithm of B_{df} were about 8.11 and 9.15 for armchair activated carbon and zigzag activated carbon, respectively, suggesting that the adsorption probabilities of mercuric oxide clusters are at least $10^{8.11}$ and $10^{9.15}$ times greater than that of SO_2. These values are obviously far larger than the volume fraction advantage of SO_2 over the mercuric oxide clusters ($10^{2.70}$–$10^{5.24}$). Therefore, taking into account the adsorption energies and concentration factors obtained from thermodynamic analysis and competitive adsorption analysis, we can conclude that there is barely any competition for adsorption sites between mercuric oxide clusters and SO_2 in flue gas—almost all of the active sites on activated carbon would be occupied by mercuric oxide clusters rather than SO_2. Thus, in contrast to the adsorption of Hg^0 on carbonaceous materials, the adsorption of mercuric oxide clusters on activated carbon would be virtually unaffected by the presence of the SO_2 in flue gas. Furthermore, rather than the traditional activated carbon injection method employed for Hg^0 removal, it would be better to use Hg^0 catalytic oxidation to remove Hg^0 from flue gas in power plants that use high-sulfur coal, as this would remove the unwanted competition from SO_2 for adsorption sites and thus improve the mercury removal process.

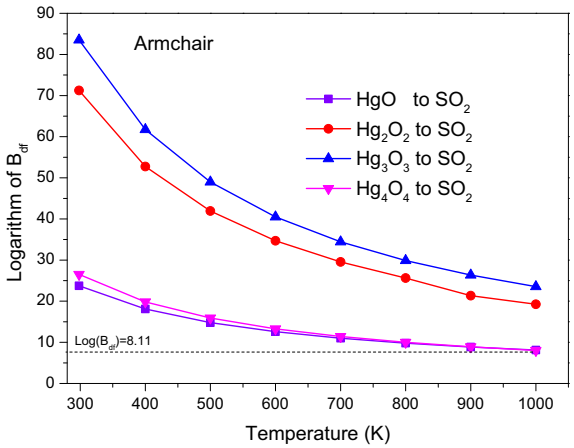

(a) Logarithm of Boltzmann distribution function for Armchair activated carbon

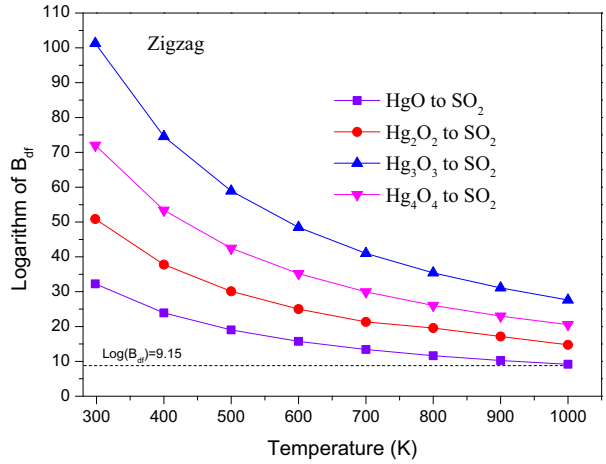

(b) Logarithm of Boltzmann distribution function for Zigzag activated carbon

Fig. 9 The logarithm of the Boltzmann distribution as a function of temperature. **a** Logarithm of the Boltzmann distribution function as a function of temperature for armchair activated carbon. **b** Logarithm of the Boltzmann distribution function as a function of temperature for zigzag activated carbon

Conclusion

To obtain a comprehensive understanding of the adsorption of mercuric oxide clusters on activated carbon, we have used density functional theory to investigate the effects of the pre-adsorption of SO_2 on the activated carbon, analyze the ESP on the activated carbon surface, probe the thermodynamics of the process, and assess the impact of competitive adsorption of mercuric oxide clusters and SO_2. Based on the results of this study, we can draw four main conclusions:

(1) The adsorption of mercuric oxide clusters on activated carbon can be categorized as chemical adsorption, as it involves high adsorption energies (exceeding −1.03 eV). This implies that activated carbon could be an excellent sorbent for removing mercuric oxide clusters from power-plant flue gas.

(2) Pre-adsorption of SO_2 by the activated carbon does not necessarily enhance the adsorption of mercuric oxides on the activated carbon due to the rather irregular distribution of ESP values on the activated carbon surface.
(3) Thermodynamic analysis suggests that the adsorption energy decreases with increasing temperature, and that the adsorption energy of SO_2 on activated carbon is lower than those of mercuric oxide clusters at a particular temperature.
(4) An investigation of the competitive adsorption of mercuric oxide clusters and SO_2 on the activated carbon indicated that SO_2 would occupy hardly any of the active sites on the unburned carbon due to strong competition from the mercuric oxide clusters. Thus, the adsorption of mercuric oxide clusters in power-plant flue gas by carbonaceous materials would not be affected by the presence of SO_2 in the flue gas.

Acknowledgements This work was supported by the Beijing Natural Science Foundation (2182066), the Natural Science Foundation of Heibei Province (B2018502067), and the Fundamental Research Funds for the Central Universities (JB2015RCY03 and 2017XS121). The provision of access to TianHe-2 supercomputer computational resources of the Lvliang Supercomputer Center is acknowledged.

Compliance with ethical standards

Conflict of interest The authors declare no competing financial interest.

References

1. Mergler D, Anderson HA, Mahaffey KR, Murray M, Stern AH (2007) Methylmercury exposure and health effects in humans: a worldwide concern. Ambio 36(1):3–11
2. Scheuhammer AM, Meyer MW (2007) Effects of environmental methylmercury on the health of wild birds, mammals, and fish. Ambio 36(1):12–18
3. Liu J, Qu W, Sang WJ, Zheng C (2012) Effect of SO_2 on mercury binding on carbonaceous surfaces. Chem Eng J 184(2):163–167
4. Tan Y, Mortazavi R, Dureau B, Douglas MA (2004) An investigation of mercury distribution and speciation during coal combustion. Fuel 83(16):2229–2236
5. He C, Shen B, Chen J, Cai J (2014) Adsorption and oxidation of elemental mercury over Ce-MnOx/Ti-PILCs. Environ Sci Technol 48(14):7891–7898
6. He P, Zhang X, Peng X, Jiang X, Wu J, Chen N (2015) Interaction of elemental mercury with defective carbonaceous cluster. J Hazard Mater 300:289–297
7. Liu J, Cheney MA, Wu F, Li M (2011) Effects of chemical functional groups on elemental mercury adsorption on carbonaceous surfaces. J Hazard Mater 186(1):108–113
8. Liu J, Qu W, Yuan J, Wang S, Qiu J, Zheng CJE, et al. (2010) Theoretical studies of properties and reactions involving mercury species present in combustion flue gases. Energy Fuels 24(1):117–122
9. Xiang F, Yong H, Kumar S, Wang Z, Liu L, Huang Z, et al. (2017) Influence of hydrothermal dewatering on trace element transfer in Yimin coal. Appl Therm Eng 117:675–681
10. Xu P, Luo G, Zhang B, Zeng X, Xu Y, Zou R, et al. (2017) Influence of low pressure on mercury removal from coals via mild pyrolysis. Appl Therm Eng 113:1250–1255
11. Gao Y, Zhang Z, Wu J, Duan L, Umar A, Sun L, et al. (2013) A critical review on the heterogeneous catalytic oxidation of elemental mercury in flue gases. Environ Sci Technol 47(19):10813–10823
12. Chu P, Laudal D, Brickett L, Lee C. Power plant evaluation of the effect of SCR technology on mercury. Conference Power plant evaluation of the effect of SCR technology on mercury. p 19–22
13. Yang W, Gao Z, Ding X, Lv G, Yan W (2018) The adsorption characteristics of mercury species on single atom iron catalysts with different graphene-based substrates. Appl Surf Sci 455:940–951
14. Feeley TJ, Brickett LA, O'Palko BA, Murphy JT (2010) Field testing of mercury control technologies for coal-fired power plants. National Energy Technology Laboratory (DOE), Washington, DC
15. Li H, Wu CY, Li Y, Zhang J (2012) Superior activity of MnO_x–CeO_2/TiO_2 catalyst for catalytic oxidation of elemental mercury at low flue gas temperatures. Appl Catal B Environ 111(3):381–388
16. Mei Z, Shen Z, Mei Z, Zhang Y, Xiang F, Chen J, et al. (2008) The effect of N-doping and halide-doping on the activity of $CuCoO_4$ for the oxidation of elemental mercury. Appl Catal B Environ 78(1–2): 112–119
17. Li J, Yan N, Qu Z, Qiao S, Yang S, Guo Y, et al. (2009) Catalytic oxidation of elemental mercury over the modified catalyst Mn/α-Al_2O_3 at lower temperatures. Environ Sci Technol 44(1):426–431
18. Xu J, Bao J, Tang J, Du M, Liu H, Xie G et al (2018) Characteristics and inhibition of Hg^0 re-emission in a wet flue gas desulfurization system. Energy Fuel 32(5):6111–6118
19. Gupta VK, Saleh TA (2013) Sorption of pollutants by porous carbon, carbon nanotubes and fullerene—an overview. Environ Sci Pollut Res 20(5):2828–2843
20. Nguyen-Thanh D, Bandosz TJ (2005) Activated carbons with metal containing bentonite binders as adsorbents of hydrogen sulfide. Carbon 43(2):359–367
21. López-Antón MA, Díaz-Somoano M, Fierro JLG, Martínez-Tarazona MR (2007) Retention of arsenic and selenium compounds present in coal combustion and gasification flue gases using activated carbons. Fuel Process Technol 88(8):799–805
22. Laumb JD, Benson SA, Olson EA (2004) X-ray photoelectron spectroscopy analysis of mercury sorbent surface chemistry. Fuel Process Technol 85(6):577–585
23. Norell M (2012) Control of mercury emissions from coal-fired electric utility boilers: interim report including errata dated 3-21-02. US EPA, Washington, DC
24. Yang H, Xu Z, Fan M, Bland AE, Judkins RR (2007) Adsorbents for capturing mercury in coal-fired boiler flue gas. J Hazard Mater 146(1):1–11
25. Pedersen KH, Jensen AD, Dam-Johansen K (2010) The effect of low-NO_x combustion on residual carbon in fly ash and its adsorption capacity for air entrainment admixtures in concrete. Combust Flame 157(2):208–216
26. Shen F, Liu J, Zhang Z, Dong Y, Gu C (2018) Density functional study of hydrogen sulfide adsorption mechanism on activated carbon. Fuel Process Technol 171:258–264
27. Gao Z, Li M, Sun Y, Yang W (2018) Effects of oxygen functional complexes on arsenic adsorption over carbonaceous surface. J Hazard Mater 360:436–444
28. Zhang H, Liu J, Shen J, Jiang X (2015) Thermodynamic and kinetic evaluation of the reaction between NO (nitric oxide) and char(N) (char bound nitrogen) in coal combustion. Energy 82:312–321
29. Rémy S, Prudent P, Hissler C, Probst JL, Krempp G (2003) Total mercury concentrations in an industrialized catchment, the Thur River basin (North-Eastern France): geochemical background level and contamination factors. Chemosphere 52(3):635–644

30. Frisch MJ, Trucks G, Schlegel HB, Scuseria G, Robb M, Cheeseman J, et al. (2009) Gaussian 09, revision D.01, vol 27. Gaussian Inc., Wallingford, p 34
31. Goerigk L, Grimme S (2010) Efficient and accurate double-hybrid-meta-GGA density functionals—evaluation with the extended GMTKN30 database for general main group thermochemistry, kinetics, and noncovalent interactions. J Chem Theory Comput 7(2):291–309
32. Neese F (2012) The ORCA program system. Wiley Interdiscip Rev Comput Mol Sci 2(1):73–78
33. Gao Z, Yang W, Ding X, Ding Y, Yan W (2017) Theoretical research on heterogeneous reduction of N_2O by char. Appl Therm Eng 126:28–36
34. Zhang H, Liu J, Wang X, Luo L, Jiang X (2017) DFT study on the C(N)-NO reaction with isolated and contiguous active sites. Fuel 203:715–724
35. Liu J, Qu W, Yuan J, Wang S, Qiu J, Zheng C (2010) Theoretical studies of properties and reactions involving mercury species present in combustion flue gases. Energy Fuel 24(1):509–518
36. Gao Z, Ding Y, Yang W, Han W (2017) DFT study of water adsorption on lignite molecule surface. J Mol Model 23(1):27
37. Lu T, Manzetti S (2014) Wavefunction and reactivity study of benzo[a]pyrene diol epoxide and its enantiomeric forms. Struct Chem 25(5):1521–1533
38. Zhang X, Zhou Z, Zhou J, Liu J, Cen K (2012) Density functional study of NO desorption from oxidation of nitrogen containing char by O. Combust Sci Technol 184(4):445–455
39. Gao Z, Yang W (2016) Effects of CO/CO_2/NO on elemental lead adsorption on carbonaceous surfaces. J Mol Model 22(7):166
40. Yang Y, Jing L, Zhang B, Feng L (2017) Mechanistic studies of mercury adsorption and oxidation by oxygen over spinel-type $MnFe_2O_4$. J Hazard Mater 321:154–161
41. Yang W, Gao Z, Liu X, Li X, Ding X, Yan WJCS, et al. (2018) Single-atom iron catalyst with single-vacancy graphene-based substrate as a novel catalyst for NO oxidation: a theoretical study. Catal Sci Technol 8(16):4159–4168
42. Gao Z, Sun Y, Li M, Yang W, Ding X (2018) Adsorption sensitivity of Fe decorated different graphene supports toward toxic gas molecules (CO and NO). Appl Surf Sci 456:351–359
43. Yang W, Gao Z, Liu X, Ding X, Yan W (2019) The adsorption characteristics of As_2O_3, Pb^0, PbO and $PbCl_2$ on single atom iron adsorbent with graphene-based substrates. Chem Eng J 361:304–313
44. Espinal JF, Mondragón F, Truong TN (2009) Thermodynamic evaluation of steam gasification mechanisms of carbonaceous materials. Carbon 47(13):3010–3018
45. Li J, Maroto-Valer MMJC (2012) Computational and experimental studies of mercury adsorption on unburned carbon present in fly ash. Carbon 50(5):1913–1924
46. Shen F, Liu J, Dong Y, Wu DJCEJ (2018) Mercury removal by biomass-derived porous carbon: experimental and theoretical insights into the effect of H_2S. Chem Eng J 348:409–415
47. Perry S, Hambly E, Fletcher T, Solum M, Pugmire R (2000) Solid-state ^{13}C NMR characterization of matched tars and chars from rapid coal devolatilization. Proc Combust Inst 28(2):2313–2319
48. Chen N, Yang RT (1998) Ab initio molecular orbital calculation on graphite: selection of molecular system and model chemistry. Carbon 36(7–8):1061–1070
49. Montoya A, Truong TTT, Mondragón F, Truong TN (2001) CO desorption from oxygen species on carbonaceous surface: 1. Effects of the local structure of the active site and the surface coverage. J Phys Chem A 105(27):6757–6764
50. Rui W, Wei F, Dandan Z, Huiling L, Huanyu Z, Xuri H (2017) Geometric stability of PtFe/PdFe embedded in graphene and catalytic activity for CO oxidation. Appl Organomet Chem 31(11):e3808
51. Olson E, Laumb J, Benson S, Dunham G, Sharma R, Mibeck B, et al. (2003) An improved model for flue gas-mercury interactions on activated carbons. In: Proceedings of 2003 Combined Power Plant Air Pollutant Control Mega Symposium. Energy & Environmental Research Center, Grand Forks, pp 19–22
52. Wang C, Xu S, Cui YP (2013) Optical and bonding characters of Hg type clusters. New J Chem 37(10):3303–3307
53. Padak B, Wilcox J (2009) Understanding mercury binding on activated carbon. Carbon 47(12):2855–2864
54. Yang FH, Yang RT (2002) Ab initio molecular orbital study of adsorption of atomic hydrogen on graphite: insight into hydrogen storage in carbon nanotubes. Carbon 40(3):437–444
55. Liu J, Qu W, Joo SW, Zheng C (2012) Effect of SO_2 on mercury binding on carbonaceous surfaces. Chem Eng J 184:163–167
56. Murray JS, Politzer P (1998) Statistical analysis of the molecular surface electrostatic potential: an approach to describing noncovalent interactions in condensed phases. J Mol Struct THEOCHEM 425(1–2):107–114
57. Hohenstein EG, Sherrill CD (2009) Effects of heteroatoms on aromatic pi-pi interactions: benzene-pyridine and pyridine dimer. J Phys Chem A 113(5):878
58. Lu T, Chen F (2012) Multiwfn: a multifunctional wavefunction analyzer. J Comput Chem 33(5):580–592
59. Serre SD, Silcox GD (2000) Adsorption of elemental mercury on the residual carbon in coal fly ash. Ind Eng Chem Res 39(6):1723–1730
60. Park J-H, Ahn J-W, Kim K-H, Son Y-S (2019) Historic and futuristic review of electron beam technology for the treatment of SO_2 and NO_x in flue gas. Chem Eng J 355:351–366